

## MAGNETICALLY TUNABLE SAW-RESONATOR

P. Smole<sup>1,2</sup>, W. Ruile<sup>2</sup>, C. Korden<sup>2</sup>, A. Ludwig<sup>3</sup>, E. Quandt<sup>3</sup>, S. Krassnitzer<sup>4</sup>, and P. Pongratz<sup>1</sup>

<sup>1</sup>Institute of Solid State Physics, Vienna University of Technology, Vienna, Austria

<sup>2</sup>EPCOS AG, Research and Development, Munich, Germany

<sup>3</sup>CAESAR, center of advanced european studies and research, Bonn, Germany

<sup>4</sup>UNAXIS Balzers AG, Balzers, Liechtenstein

**Abstract** – At present different tuning methods for acoustic devices exist. Established technologies are the integration of stricitive materials or semiconductor structures in the cavity of a delay-line or resonator. Common to all these devices is the tuning of delay time or phase by changing the electrical or mechanical surface boundary condition for the propagating surface acoustic wave (SAW).

This paper presents a completely new approach for frequency tuning. The resonance frequency of a SAW resonator is shifted by directly changing the propagation velocity of the SAW. This is achieved by altering the corresponding elastic stiffness by an external magnetic field, using a multilayer structure exhibiting Giant  $\Delta E$  effect. A sacrificial layer technique is used to realize a first experimental device, basically consisting of a piezoelectric ZnO-layer on an amorphous magnetostrictive layer of FeCo-SiB. All layers have been deposited by RF-sputtering on a 4" quartz carrier-wafer. Aluminum electrode structures were deposited subsequently in order to excite SAWs. In the measurement setup an external magnetic field between 0 to 50 Oe has been applied to the device. A tuning range of about -1.2 % and -0.9 % at center frequencies of 1.2 and 1.6 GHz could be demonstrated, respectively.

### I. INTRODUCTION

Current frequency allocations for cellular and cordless phones basically split into two regions at 1 and 2 GHz, as shown in Fig. 1.

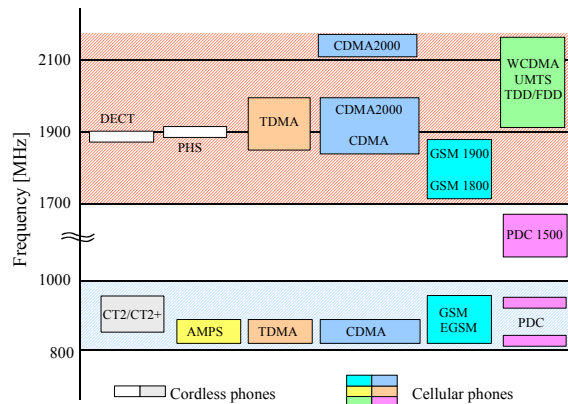


Fig. 1. Current frequency allocations for cellular and cordless phones

To cover all frequency bands of all systems within the 1 and 2 GHz region would normally require a multitude of different filters. An alternative would be the substitution of the filterbank by one single tunable filter with a tuning range of about 30 %. This tunable filter may be realized as a ladder type structure with tunable one-port resonators as shown in Fig. 2. In this paper we investigate one way to tune such a

one-port SAW resonator. In recent years different research groups already demonstrated the potential of tuning SAW devices [1-5]. Tuning of propagation velocity and thus time delay and phase was realized by integrating magnetostrictive or semiconducting layers on the surface of SAW components. However the excitation frequency of these devices remained unchanged and the achieved tuning effects were below several 100 ppm.

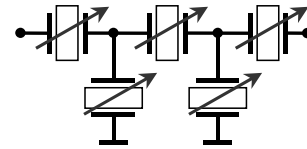


Fig. 2. Basic model of tunable ladder type filter consisting of tunable one-port resonators

We introduce a new approach to directly tune the center frequency of a SAW resonator by using a smart material with a variable Young's modulus  $E$  for SAW propagation. In the next section we will discuss the effect of an  $E$  modulus change on the frequency. In section III the physical effect behind the change of Young's modulus is outlined. The experimental setup is described in Section IV, the first results will be discussed in Section V. Section VI concludes with a resume of the results.

### II. BASIC IDEA

The frequency  $f$  of a SAW device with a pitch  $p$  (distance between electrodes) is basically defined by:

$$f = \frac{v_R}{2p} \quad (1)$$

where  $v_R$  is the velocity of the Rayleigh wave in a given material. From (1) follows that  $f$  can be changed either by altering  $p$  or  $v_R$ . The pitch  $p$ , however, is fixed during photolithographic production of the SAW device.

For reasons of simplicity in the following derivation the wave velocity  $v_R$  is assumed to be proportional to the longitudinal wave velocity  $v_L$  [6]. For nonpiezoelectric isotropic materials therefore the following equation holds:

$$v_L = \sqrt{\frac{E}{\rho}} \quad (2)$$

with  $\rho$  being the density of the material and  $E$  the Young's modulus. Hence  $v_L$  can be changed either by altering  $\rho$  or  $E$ .

A significant change of density  $\rho$ , however cannot be achieved. Therefore we finally estimate the relative change of the center frequency by expanding (1) in consideration of (2) by:

$$-\frac{\Delta f}{f} \propto \frac{1}{2} \frac{\Delta E}{E} \quad (3)$$

From (3) follows that a direct shift in center frequency is obtained by altering the E modulus of the material. Smart materials which allow such changes of elastic modulus depending on an external physical field quantity do exist and will be discussed in the next section.

### III. GIANT $\Delta E$ EFFECT

Amorphous magnetostrictive materials change their E modulus significantly if an external field is applied. This is called the Giant  $\Delta E$  effect. Fig. 3 shows schematically the change of the Young's modulus and the physical effect from hard **a** to soft **b** and back again **c** for increasing intensity of the magnetic field applied in hard axis direction.

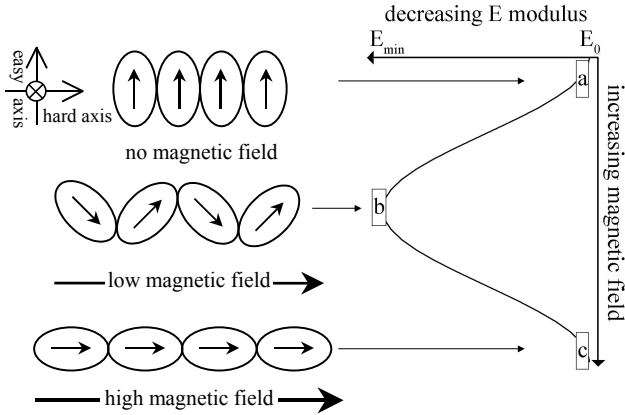


Fig. 3. Model of magnetostrictive material behavior in dependence of external magnetic field applied in hard axis direction

Cooling down magnetostrictive softmagnetic materials with an ideal spherical magnetic microstructure below Curie temperature while applying an external magnetic field leads to an induced uniaxial magnetic anisotropy i.e. an easy and a hard axis (Fig. 3 **a**). Here the easy axis is the direction where the total energy minimizes when no external field is applied. The perpendicular direction is defined by the hard axis. Applying an external field in hard axis direction leads primarily to an decrease in the elastic modulus towards a local minimum (Fig. 3 **b**). A further increase of the external field causes a proportional growth of the elastic modulus up to a saturation value where the E modulus is approximately the same as in the initial state (Fig. 3 **c**). Applying an external field in easy axis direction only causes a rotation of non-aligned magnetic moments but no further change in Young's modulus.

According to [7] the  $\Delta E$  effect (4) of a magnetoelastic material is determined by  $E_0$ , the elastic modulus at magnetic

saturation, the saturation magnetostriction coefficient  $\lambda_s$  and  $K_{tot}$  the total anisotropy ( $E_{min}$  being the minimum Young's modulus). The total anisotropy  $K_{tot}$  is the sum of the crystalline, shape, induced and magnetoelastic anisotropy contributions.

$$\frac{\Delta E}{E_0} = \frac{E_0 - E_{min}}{E_0} \propto \frac{\lambda_s^2}{K_{tot}} \cdot E_0 \quad (4)$$

To maximize the  $\Delta E$  effect, materials combining high saturation magnetostriction  $\lambda_s$  with low total anisotropy  $K_{tot}$  are needed. Due to the almost vanishing crystalline anisotropy and the reduction of the internal stress state by a temperature annealing process, amorphous magnetostrictive materials like FeCoSiB are promising for a high  $\Delta E$  effect. Effects of more than 30 % for thin films [8] and more than 100 % for ribbons [9] are reported. Therefore the required frequency change of 30 % according to (3) should be feasible.

### IV. EXPERIMENTAL

A first experimental SAW device has been realized using a sacrificial layer technique. This method seems to be advantageous to obtain highly c-axis oriented ZnO and to prevent the recrystallisation of the amorphous magnetoelastic layer. A detailed description of this technique will be given elsewhere [10]. Fig. 4 depicts the resonator layout and a cross section through the multilayer system, schematically. The multilayer structure consists of a piezoelectric ZnO-layer on an amorphous magnetostrictive layer with the chemical composition  $(\text{Fe}_{90}\text{Co}_{10})_{78}\text{Si}_{12}\text{B}_{10}$  adhesively bonded on 4'' XT-cut quartz carrier wafers. An additional Chromium layer is deposited between the ZnO and FeCoSiB to enhance adhesion. All films were deposited using a RF magnetron sputtering system.

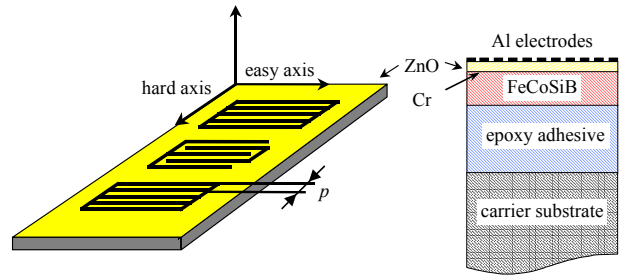


Fig. 4. Basic resonator layout and cross section of the multilayer system

FeCoSiB exhibits a saturation magnetostriction  $\lambda_s$  up to 35 ppm with simultaneous low total anisotropy [8]. To achieve an in-plane magnetic easy axis of the magnetic layer, as shown in Fig. 4., an in-plane magnetic field of 100 Oe was applied during deposition.

The aluminum electrodes were deposited by physical vapor deposition and structured using a photolithographic process so that the SAW propagation direction is aligned parallel to the magnetic hard axis direction. All processes were carried

out well below Curie temperature of the magnetic material ( $\sim 400^\circ\text{C}$ ) to sustain the induced magnetic properties.

A one-port resonator design with 100-50-100 electrodes for the reflectors and interdigital transducer respectively, was realized. Two different designs with pitches  $p$  of 0.8 and 1.1  $\mu\text{m}$  were used to excite SAWs on the multilayer system at center frequencies of 1.2 and 1.6 GHz, respectively.

The one-port resonators were measured on wafer level with a hand operated wafer prober using a Rhode&Schwarz ZVC network analyzer. Helmholtz coils were used to generate the magnetic field. To ensure a homogeneous magnetic field distribution the whole test setup is constructed using non-magnetic materials. The magnetic field strength was measured using a NVE Giant magnetoresistive sensor mounted on one of the probes directly above the wafer. While cycling the magnetic field a transmission measurement of the one-port resonator was carried out (Fig. 5). By deembedding the contact resistance and parasitic effects were separated from measurement data.

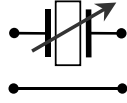


Fig. 5. Transmission measurement for tunable one-port resonator

## V. RESULTS AND DISCUSSION

Fig. 6 shows the measured absolute value of the real part of the admittance  $Y_{12}$  against the external magnetic field applied in hard axis direction.

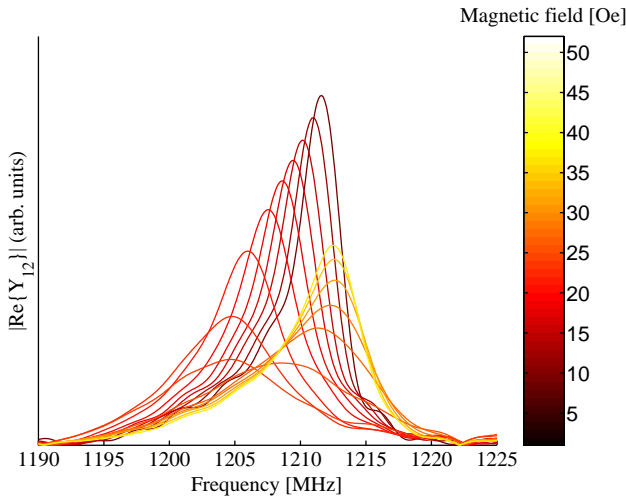


Fig. 6. Real part of  $Y_{12}$  as a function of applied field in hard axis direction at a center frequency of 1.2 GHz,  $p = 1.1 \mu\text{m}$

A decrease in center frequency is observed with the increase of the magnetic field. The concurrent broadening of the resonance indicates an increase of damping effects. From the maximum in the real part of the admittance function the relative change in center frequency is determined. The quality factor  $Q$  is calculated according to (5) from the 3dB bandwidth. Fig. 7 shows the expected correlation according

to Section 3 between the change of Young's modulus and the frequency against the external field applied in hard axis direction.

$$Q = \frac{f}{\Delta f|_{3\text{dB}}} \quad (5)$$

A direct proportionality of damping effects in terms of the quality factor and change in phase velocity and thus the frequency can be shown experimentally. This correlation was already reported before e.g. in [11] where a sinusoidal dependence from the double-angle between SAW propagation and intrinsic magnetic field direction is derived for the damping effects. As a consequence the maximum damping occurs when this angle equals to  $45^\circ$  i.e. the minimum of Young's modulus and the maximum of the frequency shift.

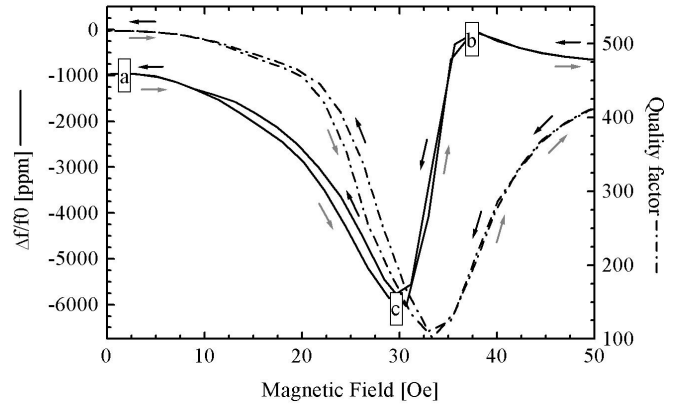


Fig. 7. Relative frequency change and quality factor as a function of applied field in hard axis direction at 1.6 GHz,  $p = 0.8 \mu\text{m}$  (increasing field direction indicated by gray arrows, decreasing field indicated by black arrows)

The magnetic field in Fig. 7 and Fig. 8 is marked by gray and black arrows for increasing and decreasing magnitude, respectively. In Fig. 8 the relative frequency change and quality factor with respect to the external magnetic field applied in easy axis direction is shown.

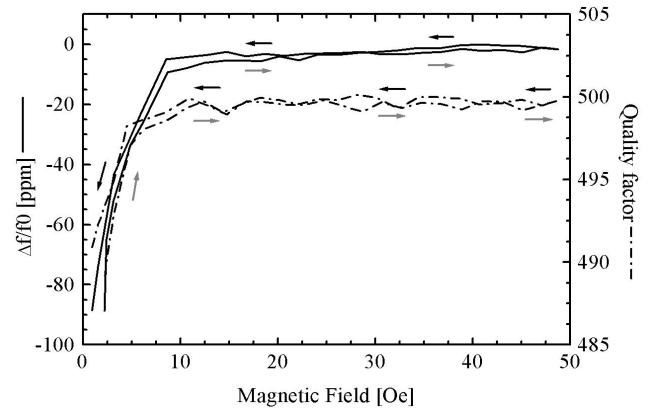


Fig. 8. Relative frequency change and quality factor as a function of applied field in easy axis direction at 1.6 GHz,  $p = 0.8 \mu\text{m}$  (increasing field direction indicated by gray arrows, decreasing field indicated by black arrows)

The small change in frequency is caused by the flip process

of the nonaligned magnetic moments in the external field direction.

TABLE 1 summarizes the results for the realized samples. The given values of the achieved tunability are mean values and taken from repeated measurements of 20 samples. The deviation between the best sample and the mean value in tunability is due to cross wafer inhomogeneities in layer thicknesses and magnetostrictive properties.

TABLE 1  
mean value of tunability and best sample result

pitch [ $\mu\text{m}$ ]	$f_0$ [GHz]	mean value $\Delta f/f_0$ [%]	best sample $\Delta f/f_0$ [%]
0.8	1.65	$-0.62 \pm 0.03$	-0.86
1.1	1.21	$-0.82 \pm 0.04$	-1.21

The deviation in the tunability for the two frequencies can be explained by the penetration depth of the SAW. Finite element simulations of this multilayer system reveal that for shorter wavelengths a major part of the mechanical energy is travelling in the piezoelectric layer and not in the magnetostrictive layer. Fig. 9 shows the relative frequency change against the relative E modulus change for the above described SAW samples. With increasing pitch at a fixed layer system the relative piezoelectric layer thickness decreases and therefore the achievable tunability at given  $\Delta E$  effect increases.

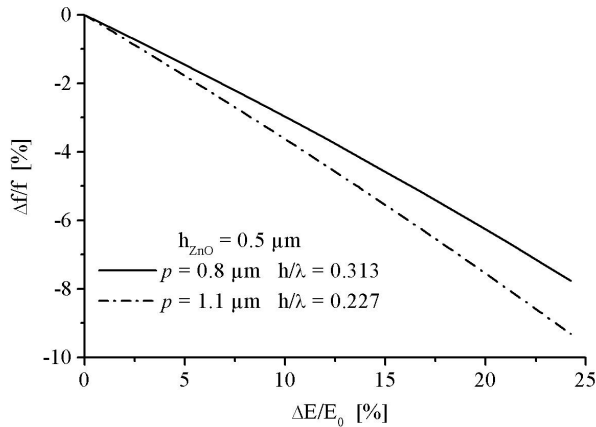


Fig. 9. Relative frequency change as a function of the relative change in E modulus

Hence to maximize the tunability the piezoelectric layer thickness has to be reduced. A limiting factor for this reduction is the achievable effective piezoelectric coupling which essentially decreases proportional to the piezoelectric layer thickness [12].

Our first experimental devices showed tunabilities of about -1 % which is far better than those achieved up to now, but still not sufficient for the application in tunable filters. Furthermore the attenuation of the resonance due to magnetic effects is still too high. To increase the tunability the magnetostrictive layer may be optimized by temperature annealing treatments in an external magnetic field, enhancing the  $\Delta E$

effect. The reduction of ZnO layer thickness is also a promising possibility to increase the tuning effect. The reduction of damping effects by application of magnetostrictive multilayer systems have already been reported [13].

## VI. CONCLUSION

Tunable filters would be desirable for mobile phone applications in order to cover the required frequency allocations with a minimum number of filter components.

In a first approach the feasibility of tuning the center frequency of a one-port resonator using  $(\text{Fe}_{90}\text{Co}_{10})_{78}\text{Si}_{12}\text{B}_{10}$  as a smart material for SAW propagation was demonstrated. First experimental devices showed a maximum tuning range of -1.21% and -0.86 % at center frequencies of 1.2 and 1.65 GHz, respectively, by changing the external magnetic field applied in hard axis direction between 0 and 50 Oe. A direct relation between the magnitude of tuning effect and the quality factor was observed experimentally in agreement with [11]. The dependence of the tuning effect on frequency for a fixed multilayer structure was explained by FEM simulations.

## REFERENCES

- [1] V. Koeninger, Y. Matsumura, H. H. Uchida and H. Uchida, "Surface acoustic waves on thin films of giant magnetostrictive alloys," *J. Alloys and Compounds*, 1994.
- [2] W. P. Robbins and A. Hietala, "A simple phenomenological model of tunable SAW devices using magnetostrictive thin films," *IEEE Trans. Ultrason. Ferroel. Freq. Contr.*, vol. 35, pp. 718-22, 1988.
- [3] M. Rotter, A. Wixforth, W. Ruile, D. Bernklau and H. Riechert, "Giant acoustoelectric effect in GaAs/LiNbO<sub>3</sub>/hybrids," *Appl. Phys. Lett.*, vol. 73, pp. 2128-30, 1998.
- [4] D. C. Webb, D. W. Forester, A. K. Ganguly and C. Vittoria, "Applications of amorphous Magnetic-Layers in Surface Acoustic Wave Device," *IEEE Trans. Magn.*, vol. 25, pp. 1410-1415, 1979.
- [5] M. Yamaguchi, K. Y. Hashimoto, H. Kogo and M. Naoe, "Variable SAW delay line using amorphous TbFe<sub>2</sub> film," *IEEE Trans. Mag.*, vol. 16, pp. 916-918, 1980.
- [6] D. Royer and E. Dieulesaint, *Elastic Waves in Solids I*, 1 ed. Berlin: Springer Verlag, 1999.
- [7] R. M. Bozorth, *Ferromagnetism*, 6 ed. Princeton, NJ: Van Nostrand, 1961.
- [8] A. Ludwig and E. Quandt, "Optimization of the Delta E effect in thin films and multilayers by magnetic field annealing," *IEEE Trans. Magn.*, vol. 38, pp. 2829-31, 2002.
- [9] K. I. Arai and N. Tsuya, "Magnetomechanical coupling and variable delay characteristics by means of  $\Delta E$  effect in iron-rich amorphous ribbon," *J. Appl. Phys.*, vol. 49, 1978.
- [10] P. Smole, W. Ruile, C. Korden, A. Ludwig, S. Krassnitzer and P. Pongratz, "Fabrication Techniques for Tunable SAW Resonators on Giant  $\Delta E$  Layers," unpublished.
- [11] D. Walikainen, R. F. Wiegert and M. Levy, "Magnetic field dependence of 600 MHz SAW velocity changes for thin Ni films," *IEEE Ultrason. Symp. Proc.*, 1988.
- [12] P. Smole, W. Ruile and P. Pongratz, "Characterization of Surface Acoustic Wave Propagation in a ZnO Layer on a Conducting Substrate," *IEEE Proc. Ultrason. Symp.*, 2002.
- [13] M. Inoue, N. Fujita, Y. Tsuboi and T. Fujii, "Diminution of micro-eddy-current losses in magneto-surface-acoustic-wave propagation utilizing multilayered magnetostrictive film separated by insulating layers," *Jap. J. App. Phys.*, vol. 27, pp. 169-71, 1988.